Applied Catalysis B: Environmental 115–116 (2012) 38–44

Contents lists available at SciVerse ScienceDirect

Applied Catalysis B: Environmental

journal homepage: www.elsevier.com/locate/apcatb

Review

Solar photocatalysis treatment of phytosanitary refuses: Efficiency of industrial photocatalysts

Gael Plantard[a,*], Thomas Janin[a,c], Vincent Goetz[a], Stephan Brosillon[b]

[a] Laboratoire PROcédés, Matériaux et Energie Solaire, PROMES-CNRS UPR8521, Rambla de la Thermodynamique, Tecnosud, 66100 Perpignan, France
[b] Institut Européen des Membranes, Université de Montpellier 2, ENSCM, CNRS UMR 5635, 2 place Eugène Bataillon, 34095 Montpellier Cedex, France
[c] Société Résolution, Espace Entreprises Méditerranée, Plein Sud Entreprises, 66600 Rivesaltes, France

ARTICLE INFO

Article history:
Received 7 October 2011
Received in revised form
17 November 2011
Accepted 18 November 2011
Available online 6 December 2011

Keywords:
Solar photocatalysis
Pesticides
Photocatalyst efficiency
Kinetic model

ABSTRACT

In the field of advanced oxidization processes based on solar radiation, heterogeneous solar catalysis involves exciting a photocatalyst with UV rays and one of the major problem encountered is optimizing the use of the sunlight. Catalysts in suspension develop the best ability to degrade polluting molecules. In this study, two TiO_2 catalysts in suspension which develop the best ability to degrade polluting molecules, with a granulometric ratio of 1000, have been investigated. All the experiments were performed under natural sunlight in a photoreactor consisting of three identical but independent reactors. A simple kinetic model of degradation is purposed for the media each in its optimal configuration, considering the irradiation, the catalyst and pollutant concentrations. First of all, we show that the kinetics of degradation decline as a function of the quantity of photons used and that the two catalysts (with a granulometric ratio of 1000), achieved similar performances when they were used in their optimal configurations. Secondly, the logarithm of the concentration of pyrimethanil decreased linearly as a function of the combination $Q_{UV} C_{TiO_2}^{m}$. This indicates the direct dependence of the quantity degraded on the quantity of UV energy effectively available for the photocatalytic reaction.

Contents

1. Introduction

Among the top 10 problems confronting humanity in the next decades, an energy crisis and environmental pollution come first and foremost on the list. Access to drinking water and, more generally, water management, have become major issues. Biological processes for water treatment have become the most widely used thanks to their moderate cost and simplicity. Nevertheless, several families of pollutant are not susceptible to biological treatment due to their high toxicity. Consequently, over the last 30 years additional methods have been investigated, including advanced

* Corresponding author. Tel.: +33 612524782; fax: +33 468682213.
E-mail address: plantard@univ-perp.fr (G. Plantard).

0926-3373/$ – see front matter © 2011 Elsevier B.V. All rights reserved.
doi:10.1016/j.apcatb.2011.11.034

oxidation processes (AOP). For some AOPs, their high level of energy consumption or the use of chemicals required makes them uncompetitive. The photochemistry induced by light activation triggers the formation of hydroxyl radicals, thus enabling species resistant to bioprocesses to be broken down and mineralized [1–6]. The degradation of several families of pollutants has been studied and has given promising results [7–12]. Also, the solar detoxification of hazardous dyes has demonstrated the efficiency of solar techniques [11–16].

In contrast to UV lamps, which provide an intense and constant beam, sunlight is particularly weak in the ultraviolet spectral region. This region, including A–B ultraviolet, corresponds to only 5% of the total available solar flux at the surface of the Earth. This represents a maximum irradiation available for the solar catalytic process of 50 W_{UV} m^{-2}. In this context, it is clear from studies that one of the major problems encountered in the field of advanced oxidization processes based on solar radiation is optimizing the use of the sunlight. Many studies give different kinetic model for the degradation by photocatalysis [3–14]. This great heterogeneity comes in particular from the design of the photoreactor which are very different. Indeed, according to the reactors, the optical length is different. However the kinetic of degradation is strongly correlated with the optical length and the mass of catalyst in suspension. For a given reactor and photocatalyst, there is an optimal catalyst mass beyond which it is useless to operate [7–10,17–26]. The optimal catalyst mass corresponds to the conditions for which the interception of the photons is maximum (taking account of the scattering phenomena). The literature shows that photocatalysts in the form of powdered nanoparticles in suspension have a much greater ability to degrade polluting molecules than classic two-dimensional media [18–26]. Effectively, since suspensions are dispersed evenly, they provide a material–irradiation interface throughout the whole reactor. However, their application on an industrial scale is complex and costly because it involves setting up a filtering process to separate the solid and liquid phases. This context highlighted the importance of understanding the behavior of supported catalysts effective in harnessing and using sunlight.

The present work focuses on the active molecule of the fungicide pyrimethanil often used in agriculture. Pyrimethanil is a fungicide belonging to the anilino-pyrimidines family. Studies of the photocatalysis of this substance are rare in the literature [27,28]. The first novelty in this study lies in the comparison of the efficiency of two photocatalysts in suspension using a new solar photoreactor made up of three identical flat solar reactors (no concentrating). This implementation allows the study of the influence of various parameters on the kinetics of degradation under the same conditions of solar irradiation which is variable by definition. A pseudo-first-order model was used to handle and compare the active molecule's kinetics of degradation. The optimal mass of catalyst was determined by using an original method using an optical experimental setup [7–10,21,25,29]. The form given to the catalysts and their properties, such as particle size, were studied to ascertain the performance of the various media within the context of the solar photocatalytic process. The use a photocatalyst in suspension with the same chemical composition and cristallinity than the P25 (20 nm) but with very large size (20 μm) [8–10,15,16] has been studied. This kind of photocatalyst permits an easy separation from the liquid and removes the concern on the hazardous of the nano particles for health and environment. The second novelty in this study is the optimization of the concentration of the catalyst in suspension and the ability of the suspension to absorb the light. Based on the light transmission, a kinetic law of the degradation depending of the intensity, the catalyst concentration and the pollutant concentration is obtained.

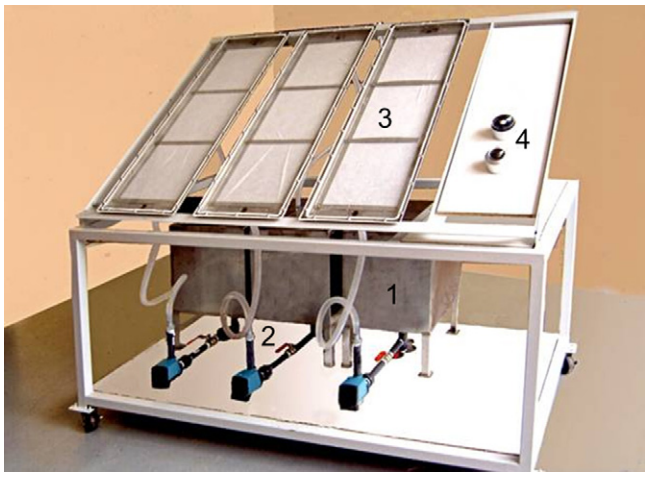

Fig. 1. Photograph and basic process design of the solar photocatalysis set-up comprising: one 50-L tank (1); an effluent recycling loop (2); a light-sensitive and -active surface (3) cover with PMMA for harnessing the solar radiation; sensors (4).

2. Experimental

2.1. Chemicals and materials

In its commercial form, available as a solid or as a liquid in concentrated suspension, there are 400 g l^{-1} of pyrimethanil. In the commercial solution the purpose of additives of unknown composition is to improve the efficacy of the active molecule, its assimilation by insects and its solubility.

The photocatalyst was TiO_2, the material most widely used for the photocatalysis. In this study, two TiO_2 Aeroxides (Degussa) differing in their granulometry were used. P-25 (BET: was 54 m^2 g^{-1}; average particle diameter: 20 nm) was taken as the reference medium on account of its photocatalytic efficiency [8–10,18–20]. A second TiO_2 (VP), Aeroperl (average particle diameter: 20 μm), was also used. The granulometric ratio between the two catalysts was 1000.

2.2. Solar photocatalytic reactor

All the experiments were performed under natural sunlight in the photoreactor shown in Fig. 1. In order to multiply the experiments in different working conditions (flow rate, concentration, media) under the same solar irradiation, an original prototype consisting of three identical but independent reactors was designed and setup. Each reactor consisted of a flat solar "panel" – the simplest geometry (Fig. 1) – with the following dimensions: 30 cm wide, 100 cm long and 2 cm thick (optical length). The volume treated was 15 l at a flowrate of 13 l min^{-1}. Water pollutants were stored in a tank (stainless steel, maximum volume 50 l). The effluent was pumped to the reactor inlet and then recirculated to the tank: the system operated in a batch mode. A mixing pump inside the tank ensures a homogeneous concentration of particles in the solution. The flow passed through each reactor from the bottom up and the whole reactor was filled by water (2 cm in depth). In these conditions, overall reactor volume was 6 l. The panels were oriented southward at an angle of 42° with respect to the horizontal, this position maximising the average solar irradiation on the panel throughout the year. Furthermore, to prevent evaporation of compounds and to ensure that the reactors remained waterproof, they were covered by a special polymethyl methacrylate (PMMA) which transmits UV radiation. The intensity of UV radiation was reduced by of about 15% by the PMMA. The measurement of the kinetics of degradation was carried out at an initial pyrimethanil

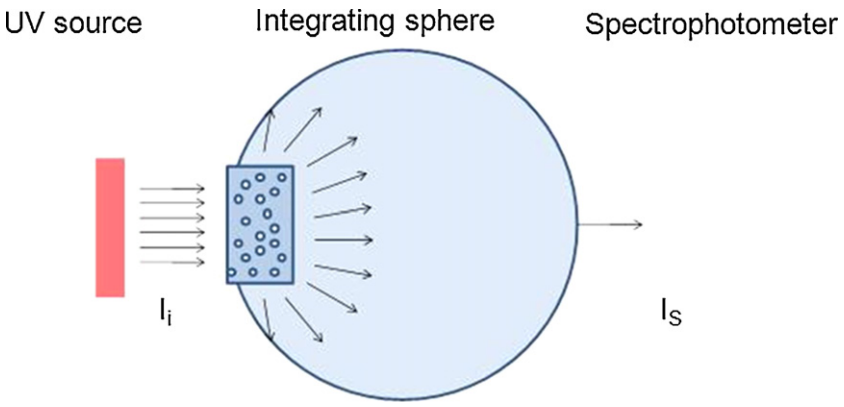

Fig. 2. Setup for measuring the rays transmitted through a quartz cell containing the catalyst in suspension. An integrating sphere collecting the sunlight is connected to a spectrophotometer permitting the measurement of both direct and diffuse rays.

concentration of 15 mg l^{-1}. 15 l of the standardized solution was introduced into a 30 liters tank and stirred continuously. To monitor the solar UV radiation, a UV radiometer (UVA-Sensor CT-UVA 3) was mounted at the same angle as the photocatalytic reactor (42°) (Fig. 1). The wavelength range was 315–400 nm.

2.3. Characterization

The evolution of the concentration of pyrimethanil was monitored during experiment by HPLC with reverse-phase liquid chromatography equipped with UV detection (JASCO UV-970M) using an Inertsil ODS-3 AIT column (25 cm × 0.46 cm). The mobile-phase composition and wavelength were acetonitril/ultra-pure water/trifluoroacetic acid at 60/40/0.05 ratio (v/v/v) at 284 nm. The high-pressure pump was a Merck L-6000 and the automatic syringe a Spark Holland MIDAS.

The optical properties of the suspensions were ascertained using an optical experimental setup (Fig. 2). The light was supplied by a source simulating solar radiation (1000 W m^{-2}, solar spectrum AM1.5). A support was used for positioning the media at the inlet of the integrating sphere, making possible the collection of the direct radiation as well as the scattered radiation transmitted [7,10,11,15,16,18–22]. The integrating sphere was coupled to a spectrophotometer obtaining a spectrum of wavelengths ranging from 250 to 1.100 nm (ultraviolet, visible, near-infrared). The catalyst in a powder form were put in suspension at different concentrations. The quartz container (optical length: 20 mm) is filled with the suspension. Then, the quartz cell was placed on the experiment's optical set up. The measurement of the transmission of light by the suspension gave the catalyst absorbency at a given concentration. By measuring the transmission of the suspension at different concentrations of TiO_2, the correlation could be determined between the transmission and the concentration of TiO_2 [21–23,25]. This method is used by Cassano [23] in the case of a P25 powder suspension.

3. Results and discussions

3.1. Preliminary experiments: adsorption, photolysis, photocatalysis

Preliminary experiments were carried out to determine the quantity of matter and, therefore, the quantity of the active molecule adsorbed on the surface of each photocatalysts and on the various surfaces involved in the process (wall of the reactor, pipes, . . .), as well as the photolysis effects likely to contribute to the degradation of the active molecule. An initial three successive stages experiment was undertaken: the first stage took place at ambient temperature and without radiation; the second with radiation; and the third under ultraviolet radiation with the P-25 catalyst in suspension. Stage 1 in Fig. 3 shows the sorption kinetics of the active substance over time. Equilibrium was reached after several hours and only 8% of the active molecule was adsorbed. Stage 2 of the experiment involved irradiating the active molecule in solution in the complete absence of the catalyst. Photodegradation of the active molecule of the order of 14% occurs after 48 h of irradiation. This degradation, attributable to the photolysis of the molecule, was due to the direct interaction of the irradiation and the active substance. In fact, as Fig. 4 shows, the spectra of solar radiation and the molecule of pyrimethanil partly coincided, indicating that photolysis of the pyrimethanil did occur. In stage 3, the catalyst, P-25 in suspension, was mixed with the solution containing the pollutant molecule subjected to irradiation. A rapid, very obvious reduction in the concentration of the pollutant shows that very significant degradation by solar photocatalysis tooks place. Thus, in comparison to the mechanism of photocatalytic degradation, the kinetics of sorption and photolysis were negligible.

The data obtained from experiments using sunlight which is a discontinuous source whose radiation varies in intensity (cloud cover) and composition (direct or diffuse). To eliminate such intermittences, the results are expressed as a function of accumulated

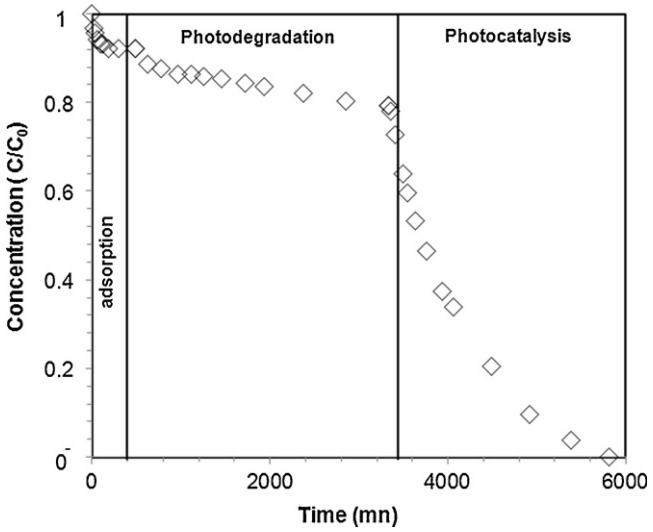

Fig. 3. Evolution of the concentration of pyrimenthanil during successive stages: (1) sorption of the pyrimenthanil by the photocatytic medium; (2) photodegradation by UV radiation; (3) solar photocatalysis activated by the P-25 catalyst.

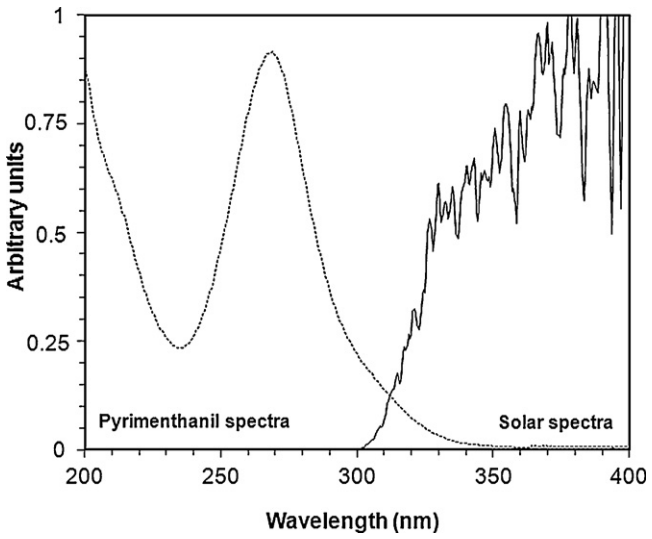

Fig. 4. Absorption spectrum of the active molecule contained in the solution (. . .) and the UV part of the AM1.5 solar spectrum (—).

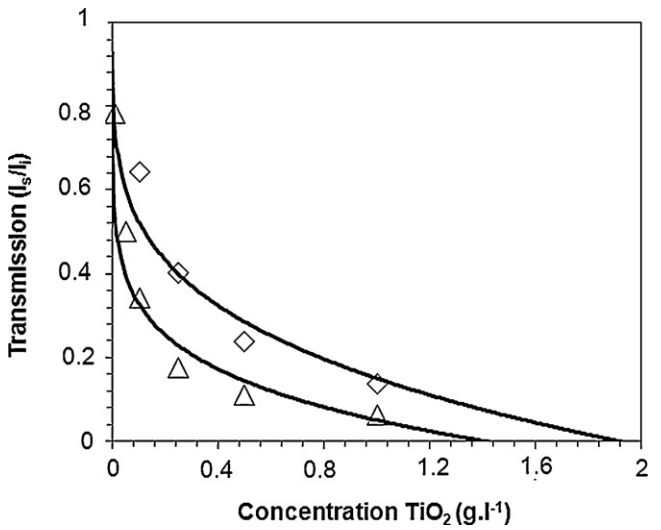

Fig. 6. Variation in the transmission of the sunlight as a function of the concentration of the catalyst in suspension: P-25 (△) and VP (◊). The curves have been established by Eq. (1).

UV energy received by each reactor per unit volume of solution to be treated (Eq. (1)). This expression, a slightly modified form of Goslich et al. [30], is commonly used when working with the solar resource. This dimension makes possible the comparison of degradation kinetics for different operating conditions (irradiated surface and reactor volume) regardless of the weather conditions and the resulting solar irradiation.

$$Q_{UV} = \frac{S}{V_T} \cdot \int_0^t I(t)\,dt \quad (1)$$

where Q_{UV} is the quantity of UV energy ($J\,m^{-3}$) harnessed by the process [5,16,23], I the UV radiation intensity ($W\,m^{-2}$) measured by the radiometer, S the irradiated surface area (m^2), V_T the reactor volume (m^3), and t is the duration of irradiation (s).

The kinetics of photolysis and of degradation by photocatalysis were determined for two concentrations of pyrimethanil (Fig. 5). The degradation kinetics as shown, recorded after a preliminary sorption stage, are given as a function of the amount of UV energy accumulated per unit volume within the process. What emerges is

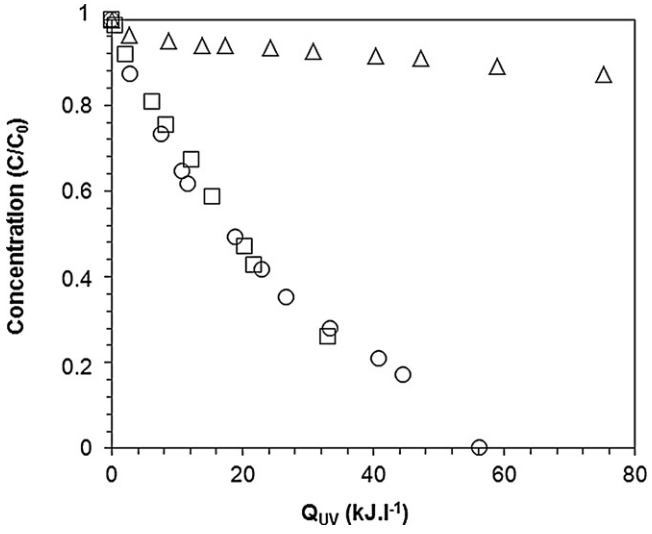

Fig. 5. Kinetics of degradation of the active molecule by photolysis (△) and photocatalysis for two initial concentrations of pyrimenthanil: 16 mg l^{-1} (□) and 23 mg l^{-1} (○).

that, firstly, direct photolysis of the molecule was very poor and, secondly, the photocatalysis kinetics obtained for the two concentrations display the same profile.

3.2. Implementation of the photocatalysts

3.2.1. Optimal mass of photocatlyst – optical set up

The ultimate purpose here was to compare the efficiency of commercial catalysts in suspension. The catalysts chosen were Degussa P-25, considered as the reference in terms of efficacy, and the catalyst VP. To compare the efficiency of the two types of powder it was necessary to determine the optimum concentration of TiO_2, meaning the concentration required to ensure the complete harnessing of the solar radiation received. The concentrations studied ranged from 0.01 g l^{-1} to 6 g l^{-1} for Degussa P-25 and from 0.1 to 10 g l^{-1} for VP Aeroperl. All solutions were first ultra sonicated (20 mn) in order to limit the aggregation of particles and stirred to avoid any decantation of the catalyst. The suspensions of the catalyst were then put inside a quartz cell on the optical apparatus (Fig. 2). The transmission, defined as the relationship between the transmitted intensity I_s over the received intensity I_i, is shown in Fig. 6 as a function of the concentration of the catalyst in suspension. The shapes of the curves representing the transmission, obtained for the two types of TiO_2, are very similar. Nevertheless, it needed a greater quantity of the VP Aeroperl compared to the Degussa P-25 to absorb the same amount of light for a given thickness. The absorption capacity of the P-25 catalyst was therefore greater than that of the VP Aeroperl. This fact is related to the size of the particles of TiO_2. Indeed, VP Aeroperl powder, which is composed of large particles (20 μm), developed a weaker specific surface than the P25 (20 nm). The ability to absorb is dependent on the surface developed. In Fig. 6, the curves for transmission are fitted by a suggested law, depending on the concentration of the catalyst (Eq. (2)).

$$T = \frac{I_s}{I_i} = 1 - \varepsilon(l \cdot C_{TiO_2})^m \quad (2)$$

where l is the cell length (cm), C_{TiO_2} the concentration of catalyst in the cell (mg l^{-1}), ε the coefficient of attenuation of the catalyst ($l\,cm^{-1}\,mg^{-1}$)$^{-m}$, m the parameter characteristic of the size and shape of the catalyst particles, I_i the flux of incident light ($W\,m^{-2}$), and I_s is the flux of light measured ($W\,m^{-2}$).

Table 1
Optical properties and characteristic kinetics of the catalysts employed.

Media	ε ($l\,g^{-1}$)$^{-m}$	m	α ($l\,kJ^{-1}$)	d (μm)
P-25	0.85	0.15	0.39	0.02
VP	0.95	0.25	0.31	20

The parameters ε and the exponent m are characteristics of the size and shape of the catalyst. They determine the extent of the surface area capable of harnessing the radiation. These two parameters, deriving from the transmission curves on the basis of Eq. (2) (Fig. 6), are shown in Table 1. The law represents transmission as a function of the concentration of the catalyst fit well the experimental results. The total absorption of the radiation received, determined by the interception of the modeled curves with the x axis, should occur for the following concentration: 1.5 g l^{-1} for the P-25 and 2 g l^{-1} for the VP.

Once the optimal mass of catalyst determined via the optical method, it is necessary to corroborate this results with the experimental kinetic data obtain in the solar photoreactor. The literature has amply shown that the rapidity with which a pollutant is degraded and mineralized by sunlight depends on numerous factors (pH, concentration of oxygen,) of which the main ones are: the concentration of the pollutant, the intensity of the impacting irradiation and the quantity of light absorbed, which is itself dependent on the concentration of the catalyst. A large number of laws appear in the literature but it emerges that a first-order kinetic can be representative of the degradation of the pollutant like pesticides.

In Fig. 7, the degradation kinetics obtained from the several concentrations of the P-25 catalyst are shown as a function of the quantity of UV energy received. The concentration decreased as a function of the quantity of UV energy received: the higher the concentration of TiO_2, the faster the degradation rate is important. As shown elsewhere [21–25], beyond a threshold concentration, the curves coincide, indicating that the kinetics no longer depend on the concentration of the catalyst. The kinetics obtained with different concentrations of the second catalyst (VP) show exactly the same tendency (Fig. 8): a close dependence of the kinetics on the concentration of the catalyst up to a threshold level. The thresholds reached for the two catalysts studied ranged from 1.5 to 2 g l^{-1} for the P-25 and 2–3 g l^{-1} for the VP. These results are in agreement with the threshold concentrations obtained from the

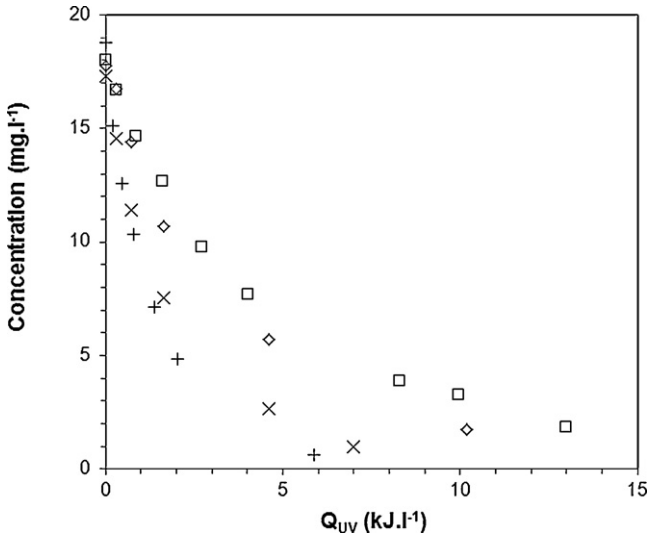

Fig. 7. Kinetics of degradation of pyrimenthanil obtained as a function of the quantity of accumulated energy for various concentrations of the P-25 catalyst: 0.05 g l^{-1} (□), 0.4 g l^{-1} (◊), 1 g l^{-1} (×), 2 g l^{-1} (+).

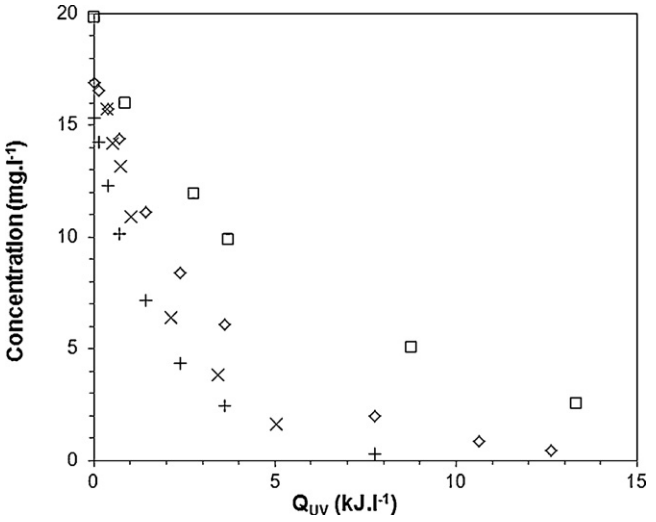

Fig. 8. Kinetics of degradation of pyrimenthanil obtained as a function of the quantity of accumulated energy for various concentrations of the P-25 catalyst: 0.5 g l^{-1} (□), 1 g l^{-1} (◊), 2 g l^{-1} (×), 3 g l^{-1} (+).

measurements of transmission (Fig. 6). Such results thus indicate that the kinetic reaches a threshold corresponding to the total use of the received radiation absorbed by the catalyst. Indeed, as has been shown in the literature [12,18–22,30], the kinetic constants of degradation obtained for a given medium depend strongly on the quantity of photons received. This implies, therefore, that degradation by photocatalysis is directly proportional to the concentration of the catalyst in suspension up to a threshold level below which all the radiation received is absorbed. Beyond this threshold concentration, a part of the catalyst in suspension is no longer irradiated: the kinetics are of the order of 0 in relation to the concentration of the catalyst. This result confirms [20–24] and highlight the possibility to use the optical set up to found the optimal mass of catalyst without additional measurements of the kinetic photodegradation.

3.2.2. Kinetic law – validation of the optimal mass

The results were treated using a pseudo first-order kinetics according the concentration of the pollutant molecule (Eq. (3)) and taking into account the intensity (I), the concentration of the catalyst (C_{TiO_2}), the irradiated surface area involved in the process (S) and the reactor volume (V_T).

$$\overset{\circ}{r} = \frac{dC}{dt} = -\alpha \frac{S}{V_T} \cdot I(t, C_{TiO_2}) \cdot C \tag{3}$$

where C is the concentration of molecule in the reactor (mg l^{-1}) and α is the photodegradation constant ($m^3\,J^{-1}$) [3,7,13,18,31].

Experiments using sunlight are subject to irregular irradiation which varies in intensity (clouds/nighttime) and in composition (UV, visible, direct/diffuse rays). When a process involves variable radiation, the intensity of the UV usable in photocatalysis corresponds to the intensity absorbed by the catalyst in suspension. The absorbed intensity is deduced by the equation for transmission (Eq. (2)) of the sunlight through a suspension of the catalyst which can be written as in Eq. (4).

$$I(t, C_{TiO_2}) = (1 - T) I_i(t) = \varepsilon (l \cdot C_{TiO_2})^m I_i(t) \tag{4}$$

where $I(t, C_{TiO_2})$ is the light absorbed (W m^{-2}) and T is the transmission of the ray through the suspension of the catalyst.

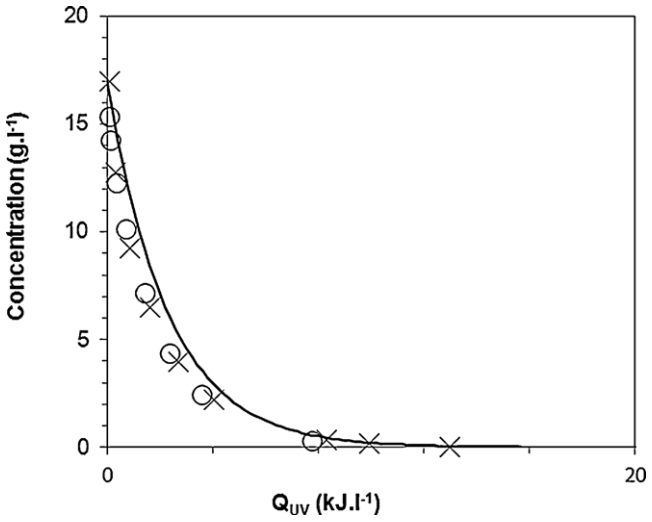

Fig. 9. Logarithm of the non-dimensional concentration (Eq. (5)), obtained as a function of tandem "quantity of accumulated energy multiplied by the concentration of the catalysts", P-25 (+) and VP (◯). The points on the graph were obtained from experiments carried out under varying conditions of irradiation, with different catalyst concentrations. The lines were obtained by Eq. (5).

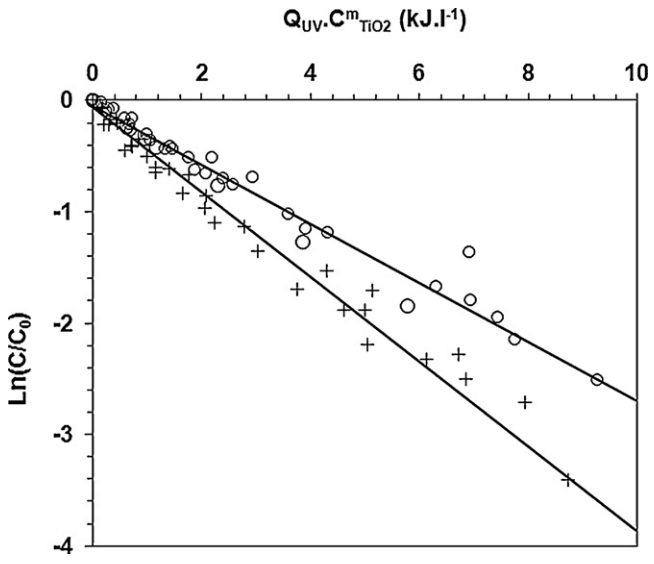

Fig. 10. Kinetics of degradation of pyrimenthanil obtained with the two media as a function of the quantity of accumulated UV energy: catalysts in suspension at a concentration of 1.5 g l^{-1} of P25 (×) and the VP (◯) at a concentration of 2.5 g l^{-1}. The lines were obtained by Eq. (5).

Integration of Eq. (4) leads to the profile of the pyrimethanil concentration as a function of the amount of UV energy accumulated (Eq. (1)).

$$\ln\left(\frac{C}{C_0}\right) = -\alpha \cdot \varepsilon (l \cdot C_{TiO_2})^m \cdot Q_{UV}(t) \quad (5)$$

The kinetics of degradation have been established for the media each in its optimal configuration, that is to say with a concentration ensuring the harnessing of the total amount of radiation received (Fig. 9). The curves representing the concentration of pyrimethanil were established taking into account the specific parameters to each medium, as expressed in Eq. (5). This simple kinetic model, it should be noted, is equivalent to the speed of degradation of the molecule that was obtained in the experiments. The model slightly underestimates the media's ability to degrade. It should be noted that the two suspended media, though differing in their granulometry, displayed similar kinetics in their optimal configurations. This result confirms the correlation between a medium's capacity to degrade molecules and its capacity to harness irradiation. It also confirms that the kinetics of degradation for the same quantity of irradiation absorbed is weakly influenced by the size of the particles. It should be emphasized that when the mass of catalyst is optimized for each photocatalyst, the efficiency of VP is comparable with the efficiency of P25. However VP is easy decanted whereas the P25 because of its nanometric size presents the drawback of a difficult solid/liquid separation.

To compare the treatment capacity of the suspended media, the amounts of pyrimethanil degraded are shown in Fig. 10 as a function of the quantity of accumulated energy multiplied by the concentration of the catalyst. The points on the graph carried out all experiments carried out under different conditions of irradiation, with various concentrations of pyrimethanil and with catalyst concentrations ranging from 0.01 to 10 g l^{-1}. The logarithm of the concentration of pyrimethanil decreased linearly as a function of the combination $Q_{UV}C^m_{TiO_2}$. The slope deduced from these lines is the product of the coefficient of attenuation and the kinetic constant ($\alpha \cdot \varepsilon$). This linear configuration indicates the direct dependence of the quantity degraded on the quantity of UV energy effectively available for the photocatalytic reaction. The kinetic constants derived from Eq. (5) are given in Table 1. It is clear that the kinetic constants for the catalysts are very close to each other. The two catalysts in suspension being constituted of the same TiO_2, they thus differ only in their granulometry. These data indicate that the performances of the media are linked to their capacity for absorbing irradiation. However, a smaller particle size of grain can absorb a greater amount of light with a smaller amount of grain due to its specific surface. Hence, to enhance the performance of the tandem medium/process, it is crucial to design supports providing a big surface area for harnessing rays or otherwise to design the process in such a way as to exploit the total amount of radiation received.

4. Conclusion

This study sought to make clear the importance of certain media for their capacity to harness solar rays to degrade pyrimethanil which is the active molecule in a fungicide. The results derive from experiments carried out on pilot-scale solar photocatalysis equipment set up to determine the performance of the media functioning in real operating conditions. The kinetics, treated by a pseudo-first-order model made it possible to compare the ability of the photocatalyst to degrade the pollutant molecule. Confirming results in the literature, the different suspensions of the medium were very effective and the kinetics depended strongly on the concentration of the catalyst. It has been shown here that the speed of degradation by solar photocatalysis is a function of certain operating parameters: the amount of the catalyst, the concentration of the pollutant, the intensity of the irradiation received. The kinetics of degradation, which are independent of the granulometry of the particles, decline as a function of the quantity of photons used, that is to say of the couple $Q_{UV} \cdot C_{TiO_2}$. The results obtained in the different conditions show that the ability to degradate molecules is correlated mainly to the quantity of photons retained. It can also be seen that the two catalysts (with a granulometric ratio of 1000), achieved similar performances when they were used in their optimal configurations. This result suggests the possibility of treating pollutants using catalysts with a large particle size which facilitates the separation stages in the post-treatment phase. These results also indicate that efforts must be directed towards developing media, either supported or in suspension, by focusing on their capacity to harness solar radiation. It is quite clear that improvements in the photocatalysis process, and particularly

in solar photocatalysis, must concentrate on optimizing the form given to the medium by developing considerable surface area for receiving radiation or, otherwise, by designing the process so that the total sum of radiation received is fully exploited.

References

[1] G.O. Shlegel, F.W. Burkholder, S.A. Klein, W.A. Beckman, B.D. Wood, J.D. Muhs, Analysis of a full spectrum hybrid lighting system, Solar Energy 76 (2004).
[2] H. Gaffron, J. Rubin, Fermentative and photochemical production of hydrogen in algae, Journal of Genetic Physiology 26 (1942).
[3] J.B. Galvez, S. Malato, Solar Detoxification, United Nations Educational Scientific and Cultural Organization, 2003.
[4] A.G. Agrios, P. Pichat, State of the art and perspectives on materials and applications of photocatalysis over TiO_2, Reviews in Applied Electrochemistry 58 (2005) 655–663.
[5] D. Robert, S. Malato, Solar photocatalysis; a clean process for water detoxification, The Science of The Total Environment 29 (2002) 85–97.
[6] D. Bahnemann, Photocatalytic water treatment: solar energy applications, Solar Energy 77 (2004) 445–459.
[7] S. Malato, P. Fernandez-Ibanez, M.I. Maldonado, J. Blanco, W. Gernjak, Decontamination and disinfection of water by solar photocatalysis: recent overview and trends, Catalysis Today 147 (2009) 1–59.
[8] S. Malato, J. Blanco, A. Campos, J. Caceres, C. Guillard, J.M. Herrmann, A.R. Fernandez-Alba, Effect of operating parameters on the testing of new industrial titania catalyst at solar pilot plant scale, Applied Catalysis B 42 (2003) 349–357.
[9] S. Malato, C. Richter, J. Blanco, M. Vincent, Photocatalytic degradation of industrial residual waters, Solar Energy 56 (1996) 401–410.
[10] S. Malato, J. Blanco, A.R. Fernandez-Alba, A. Agüera, Solar photocatalytic mineralization of commercial pesticides: acrinathrin, Chemosphere 40 (2000) 403–409.
[11] I. Oller, W. Gernjak, M.I. Maldonado, L.A. Pérez-Estrada, J.A. Sanchez-Pérez, S. Malato, Solar photocatalytic degradation of some hazardous water-soluble pesticides at pilot-plant scale, Journal of Hazardous Materials B138 (2006) 507–517.
[12] J.M. Herrmann, heterogeneous photocatalysis; fundamentals and applications to the removal of various types of aqueous pollutants, Catalysis Today 53 (1999) 115–129.
[13] P. Pichat, S. Vannier, J. Dussaud, J.P. Rubis, Field solar photocatalytic purification of pesticides-containing rinse waters from tractor cisterns used for grapevine treatment, Solar Energy 77 (2004) 533–542.
[14] L. Lhomme, S. Brosillon, D. Wolbert, J. Dussaud, Photocatalytic degradation of a phenylurea, chlortoluron, in water using an industrial titanium dioxide coated media, Applied Catalysis B 61 (2005) 227–235.
[15] G. Li Puma, P.O. Yue, A laminar failing film slurry photocatalytic reactor. Part I. Model development, Chemical Engineering Science 53 (1998) 2293–3006.
[16] S. Malato, J. Blanco, A. Vidal, C. Richter, Photocatalysis with solar energy at a pilot-plant scale: an overview, Applied Catalysis B: Environmental 37 (2002) 1–15.
[17] A.V. Emeline, V. Ryabchuk, N. Serpone, Factors affecting the efficiency of a photocatalysed process in aqueous metal-oxide dispersions. Prospect of distinguishing between two kinetic models, Journal of Photochemistry and Photobiology 133 (2000) 89–97.
[18] V. Goetz, J.P. Cambon, D. Sacco, G. Plantard, Modeling aqueous heterogeneous photocatalytic degradation of organic pollutants with immobilized TiO_2, Chemical Engineering and Processing 48 (2009) 532–537.
[19] G. Plantard, V. Goetz, F. Correia, J.P. Cambon, Importance of a medium's structure on photocatalysis: using TiO_2-coated foams, Solar Energy Materials and Solar Cells 95 (2011) 2437–2442.
[20] G. Plantard, F. Correia, V. Goetz, Kinetic and efficiency of TiO_2-coated on foam or tissue and TiO_2-suspension in a photocatalytic reactor applied to the degradation of the 2,4-diclorophenol, Journal of Photochemistry and Photobiology 222 (2011) 111–116.
[21] F. Correia, Thèse de doctorat, Université de Perpignan, Etude expérimentale et modélisation de réacteurs photochimiques solaires: performances de médias photo catalytiques, 2011.
[22] O.M. Alfano, D. Bahnemann, A.E. Cassano, R. Diller, R. Goslich, Photocatalysis in water environments using artificial and solar light, Catalysis Today 58 (2000) 199–230.
[23] A. Cassano, O.M. Alfano, Reaction engineering of suspended solid heterogeneous photocatalytic reactors, Catalysis Today 58 (2000) 167–197.
[24] A. Fernandez, preparation and characterization of TiO_2 photocatalysts supported on various rigid supports. Comparative studies of photocatalytic activity in water purification, Applied Catalysis B: Environmental 7 (1995) 49–63.
[25] F. Correia, V. Goetz, G. Plantard, D. Sacco, A model for solar photocatalytic mineralization, Journal of Solar Energy Engineering 133 (2011).
[26] G. Plantard, V. Goetz, D. Sacco, TiO_2-coated foams as a medium for solar catalysis, Materials Research Bulletin 46 (2011) 231–234.
[27] I. Oller, S. Malato, J.A. Sanchez-Pérez, M.I. Maldonado, R. Gasso, Detoxification of wastewater containing five common pesticides by solar AOPs–biological coupled system, Catalysis Today 129 (2007) 69–78.
[28] J. Arana, C. Garriga i Cabo, C. Fernandez Rodrıguez, J.A. Herrera Melian, J.A. Ortega Mendez, J.M. Dona Rodrıguez, J. Perez Pena, Combining TiO_2-photocatalysis and wetland reactors for the efficient treatment of pesticides, Chemosphere 71 (2008) 788–794.
[29] I.J. Ochuma, O.O. Osibo, R.P. Fishwick, S. Pollington, A. wagland, J. Wood, J. Winterbottom, Three-phase photocatalysis using suspended titania and titania supported on a reticulated foam monolith for water purification, Catalysis Today 128 (2007) 100–107.
[30] R. Goslich, D. Bahnemann, H.W. Shumacher, V. Benz, M. Mfiller, in: C.F. Müller (Ed.), Solar Thermal Concentrating Technologies, Proceedings of Eighth International Symposium, Köln, Germany, October 1996, Heidelberg, 1997, pp. 1337–1353.
[31] T. Oyama, A. Aoshima, S. Horikoshi, H. Hidaka, J. Zhao, N. Serpone, Solar photocatalysis, photodegradation of a commercial detergent in aqueous TiO_2 dispersions under sunlight irradiation, Solar Energy 77 (2004) 525–532.